atmosphere

Supplementary Materials: Simultaneous Quantification of Real-World Elemental Contributions from the Exhaust and Non-Exhaust Vehicular Emissions Using Road Dust Enrichment Factor-Elemental Carbon Tracer Method (EFECT)

Duran Karakaş [1,*], Ercan Berberler [1,†], Melike B. Bayramoğlu Karşı [2], Tuğçe Demir [1], Özge Aslan [3,‡], Hatice Karadeniz [3], Ömer Ağa [4,*] and Serpil Yenisoy-Karakaş [5]

Content:

Table S1. Sampling descriptions, the Bolu Mountain Highway Tunnel Study (July 23 through July 29, 2018).

Table S2. Mean concentrations of elements in the tunnel road dust samples collected in 2018 and 2019 (μg X/g road dust) and the means of road dust elemental concentration ratios to the road dust CC concentrations.

Table S3. Relative real-world elemental contributions of vehicular sources (%).

Table S4. Comparison of the relative elemental contribution results of EFECT with PMF and FA-MLR (%).

Table S5. Real-world source profiles (mass of element to tsp mass) for a mixed fleet obtained from the EFECT method and comparison with SPECIEUROPE source profiles (%).

Table S6. Comparison of exh source profiles obtained from the EFECT and SPECIATE database.

Table S7. Diagnostic ratios of selected elements for the vehicular emission sources.

Table S8. Road dust resuspension (rdrs) and exh source contributions on the TSP size OC and EC concentrations at the receptor site.

Table S9. Method detection and quantification limits (MDL and MQL) and the percent recoveries of the elements and sulfate ions.

Figure S1. Mean road dust enrichment factors of the elements in the tunnel atmosphere relative to the TSP fraction of the tunnel road dust.

Figure S2. Real-world exh source profiles (mass of element to tsp mass) for a mixed fleet obtained from the EFECT method and a comparison with the SPECIEUROPE source profiles (%).

File S1. The first stage of the EFECT: Road dust enrichment factors, EFrd (EF)

File S2. The second stage of EFECT: Exhaust EC tracer method (ECT)

REFERENCES

No. of Pages: 23

No. of Figures: 2

No. of Tables: 9

Table S1. Sampling descriptions, the Bolu Mountain Highway Tunnel Study (July 23 through July 29, 2018). .

Date	Sampling time	No. of vehicles	Vehicles/h	LDV (%)	HDV (%)	Temp (°C)	Notes
7/23/2018	11:50–13:28	1698	1040	87.2	12.8	24.5	Right lane closed
7/23/2018	13:33–15:01	1697	1157	86.6	13.4	26.5	Right lane closed
7/24/2018	10:03–11:37	1299	829	82.4	17.6	23.0	Left and center lanes are closed,
7/24/2018	11:40–13:22	1638	964	84.3	15.7	22.0	light rain for 40 min.
7/24/2018	13:25–14:58	1401	904	79.1	20.9	20.0	after 12:20.
7/25/2018	10:20–11:37	1164	907	81.7	18.3	20.0	-
7/25/2018	11:42–13:07	1420	1002	83.0	17.0	23.0	-

7/25/2018	13:10–14:37	1455	1003	78.6	21.4	23.0	Light rain
7/26/2018	09:59–11:29	1394	929	82.6	17.4	18.0	-
7/26/2018	11:34–13:10	1486	929	83.0	17.0	21.0	-
7/26/2018	13:14–14:48	1630	1040	79.6	20.4	26.0	-
7/27/2018	10:18–11:35	1156	901	84.4	15.6	20.0	-
7/27/2018	11:39–12:56	1358	1086	84.8	15.2	24.0	-
7/27/2018	12:59–14:25	1473	1028	81.6	18.4	26.0	-
7/28/2018	10:44–12:07	1813	1311	85.0	15.0	22.0	-
7/28/2018	12:10–13:49	2048	1241	86.5	13.5	22.0	-
7/28/2018	13:52–15:27	1445	913	85.6	14.4	21.0	-
7/29/2018	11:40–13:15	1921	1213	88.8	11.2	26.0	-
7/29/2018	13:17–14:54	2299	1422	89.7	10.3	27.0	-
7/29/2018	14:58–17:05	2110	1029	89.6	10.4	26.0	-
Mean		1595	1042	84.2	15.8	23.1	
Std.		312	155	3.3	3.3	2.6	

Data from our previous study [1]. The last six samples corresponded to weekend days (28-29 July). LDV: Automobiles, pick-ups, motorbikes, and minibuses; HDV: Coaches, trucks, and semi-trailer trucks.

(Table S1 continued).

Table S2. Mean concentrations of the elements in the tunnel road dust samples collected in 2018 and 2019 (μg X/g road dust) and the means of the road dust elemental concentration ratios to the road dust CC concentrations.

	2018	**2019**	**2018**	**2019**
	Mean ± Std	Mean ± Std	X/CC (2018)	X/CC (2019)
Al	36400 ± 1410	39700 ± 1550	0.783	0.783
As	16.3 ± 0.560	15.6 ± 0.542	0.000351	0.000308
Ba	327.6 ± 33.4	363.2± 33.62	0.00704	0.00716
Be	0.169 ± 0.025	0.154 ± 0.034	3.63E-06	0.00000304
Ca	27250 ± 1270	31700 ± 1650	0.586	0.625
Cd	1.125 ± 0.011	1.110 ± 0.085	2.42E-05	0.0000219
Cr	191.0 ± 51.8	209.2 ± 105.0	0.00411	0.00413
Cu	210.0 ± 16.1	224.4 ± 18.5	0.00452	0.00443
Fe	34240 ± 1670	35620 ± 2620	0.736	0.703
Mg	12400 ± 940	13270 ± 710	0.267	0.262
Mn	451 ± 14.3	487 ± 20.2	0.00970	0.00960
Ni	93.2 ± 8.60	91.0 ± 10.1	0.00200	0.00179
Pb	47.6 ± 0.65	52.7 ± 0.92	0.001024	0.000643
Sb	16.4 ± 0.798	18.7 ± 0.130	0.000352	0.000369
Sn	11.8 ± 0.389	10.6 ± 0.102	0.000254	0.000209
V	88.4 ± 3.93	90.1 ± 2.98	0.00190	0.00178
Zn	976.0 ± 18.3	987.7 ± 22.8	0.0210	0.0195
SO_4^{2-}	47400 ± 3320	50800± 2900	1.020	1.002
OC	106000 ± 7900	112500 ± 18000	2.280	2.220
EC	17600 ± 8100	20200 ± 2100	0.380	0.400
CC	46500 ± 2940	50700 ± 3800	1	1

X/CC (2018) was used as the reference ratio for the road dust enrichment factor calculations and the quantification of the *rdrs* source contribution in this study.

Table S3. Relative real-world elemental contributions of vehicular sources (%).

Element	X_{rdrs}	X_{em}	X_{exh}	$X_{n\text{-}exh}$	**Total***
Al	59.5	40.5	22.0	18.5	100.0
As	10.1	89.9	84.2	5.6	100.0

Ba	18.2	81.8	69.8	12.0	100.0
Be	4.7	95.3	93.7	1.6	100.0
Ca	63.6	36.4	18.4	17.9	100.0
Cd	14.5	85.5	76.1	9.5	100.0
Cr	7.8	92.2	88.1	4.1	100.0
Cu	35.7	64.3	46.6	17.7	100.0
Fe	44.9	55.1	39.2	15.8	100.0
Mg	66.1	33.9	17.2	16.8	100.0
Mn	62.7	37.3	20.2	17.2	100.0
Ni	15.5	84.5	75.9	8.6	100.0
Pb	16.9	83.1	71.8	11.3	100.0
Sb	13.1	86.9	79.0	7.9	100.0
Sn	8.0	92.0	87.4	4.6	100.0
V	32.3	67.7	50.6	17.1	100.0
Zn	38.6	61.4	43.6	17.8	100.0
SO_4^{2-}	9.9	90.1	84.2	5.9	100.0
OC	16.2	83.8	73.4	10.4	100.0
EC	2.9	97.1	97.1	0.0	100.0
CC	100.0	0.0	0.0	0.0	100.0

*Sum of the percentages of X_{rdrs} and X_{em} or the sum of percentages of X_{rdrs}, X_{exh}, and $X_{n\text{-}exh}$. After calculation of the elemental contributions, each sample result should be controlled first for the missing X_{tsp}, negative X_{em}, and then the negative $X_{n\text{-}exh}$ values. The elements with missing or negative values must therefore be removed completely from the X_{tsp}, X_{em}, X_{exh}, and $X_{n\text{-}exh}$ components of the corresponding samples to reach a 100% apportionment result. Since the *rdrs* contribution was calculated from the TSP concentrations of carbonate carbon (CC_{tsp}), the X_{rdrs} values should also be removed for elements with negative contributions or missing values in the dataset.

Table S4. Comparison of the relative elemental contribution results of EFECT with PMF and FA-MLR (%).

	EFECT (*rdrs + n-exh*)	**EFECT *exh***	**PMF (*rdrs + n-exh*)**	**PMF *exh***	**FA-MLR (*rdrs + n-exh*)**	**FA-MLR *exh***
Al	78.0	22.0	65.3	34.7	55.4	13.1
As	15.7	84.3	18.0	82.0		
Ba	30.2	69.8	39.0	33.0	56.0	15.3
Be	6.30	93.7				
Ca	81.5	18.5				
Cd	24.0	76.0				
Cr	11.9	88.1			40.5	6.92
Cu	53.4	46.6	99.5	0.5	93.8	0.0
Fe	60.7	39.3	71.5	28.5	66.9	0.0
Mg	82.9	17.1	61.5	38.5	55.4	19.3
Mn	79.9	20.1	67.7	32.4	65.2	0.0
Ni	24.1	75.9				
Pb	28.2	71.8	85.5	14.5	62.2	37.8
Sb	21.0	79.0	80.5	19.5	94.0	0.0
Sn	12.6	87.4	95.6	4.4		
V	48.9	51.1				
Zn	49.4	50.6	45.3	54.7		
SO_4^{2-}	15.8	84.2				
OC	26.6	73.4	61	39.0	20.0	54.8
EC	2.90	97.1	54.7	45.3	0.24	79.3

Table S5. Real-world source profiles (mass of element to *tsp* mass) for a mixed fleet obtained from the EFECT method[a] and comparison with the SPECIEUROPE source profiles (%).

	EFECT				SPECIEUROPE		
	X_{tsp}	X_{rdrs}	X_{exh}	$X_{n\text{-}exh}$	*exh+rdrs*[b]	*exh*[c]	*exh*[d]
Al	1.77 ± 0.55 (1.75)	1.09 ± 0.51 (1.06)	0.36 ± 0.41 (0.16)	0.32 ± 0.15 (0.31)	0.77	0.33	0.396
As	0.0046 ± 0.0030 (0.0046)	0.00057 ± 0.00025 (0.00058)	0.0037 ± 0.0029 (0.0038)	0.00027 ± 0.00014 (0.00023)	0.0022	0	
Ba	0.058 ± 0.017 (0.059)	0.011 ± 0.0051 (0.011)	0.041 ± 0.017 (0.039)	0.0067 ± 0.0029 (0.0062)	0.056		0.021
Be	0.000112 ± 0.00003	4.7E-06 ± 2.9E-06 (4.1E-06)	1.1E-04 ± 3.4E-05 (1.1E-04)	1.3E-06 ± 1.2E-06 (9.8E-07)			
Ca	1.34 ± 0.33 (1.36)	0.87 ± 0.39 (0.90)	0.23 ± 0.23 (0.18)	0.24 ± 0.11 (0.26)	6.07	2.38	2.98
Cd	9.1E-05 ± 4.0E-05 (9.3E-05)	3.3E-05 ± 2.0E-05 (3.5E-05)	4.2E-05 ± 3.3E-05	1.6E-05 ± 9.3E-06 (1.2E-05)	0.00114	0	0.00048
Cr	0.078 ± 0.022 (0.080)	0.0062 ± 0.0029 (0.0063)	0.069 ± 0.021 (0.069)	0.0025 ± 0.0017 (0.0022)	0.0114	0.033	0.017
Cu	0.019 ± 0.0057 (0.017)	0.0067 ± 0.0035 (0.0057)	0.0087 ± 0.0065 (0.0083)	0.0033 ± 0.0011 (0.0033)	0.15	0.32	0.019
Fe	1.25 ± 0.38 (1.08)	0.84 ± 0.45 (0.84)	0.24 ± 0.39 (0.025)	0.18 ± 0.10 (0.13)	3.75	6.2	0.54
Mg	0.53 ± 0.16 (0.54)	0.36 ± 0.18 (0.34)	0.081 ± 0.11 (0.023)	0.087 ± 0.043 (0.069)	0.53	0.79	0.18
Mn	0.022 ± 0.0059 (0.021)	0.014 ± 0.0065 (0.014)	0.0041 ± 0.0051 (0.0027)	0.0037 ± 0.0020 (0.0036)	0.047	0.049	0.015
Ni	0.011 ± 0.010 (0.0076)	0.0027 ± 0.0010 (0.0023)	0.0074 ± 0.010 (0.0026)	0.0013 ± 0.00050 (0.0015)	0.00113	0.006	0.0109
Pb	0.012 ± 0.0095 (0.0085)	0.0047 ± 0.0021 (0.0045)	0.0054 ± 0.011 (0.0010)	0.0016 ± 0.00071 (0.0014)	0.024	0.21	0.026
Sb	0.0026 ± 0.00095 (0.0026)	0.00056 ± 0.00026 (0.00059)	0.0017 ± 0.00090 (0.0019)	0.00034 ± 0.00016 (0.00030)	0.014	0	
Sn	0.0021 ± 0.00092 (0.0018)	0.00040 ± 0.00024 (0.00032)	0.0014 ± 0.00063 (0.0014)	0.00025 ± 0.00016 (0.00019)	0.032	0	
V	0.0082 ± 0.0045 (0.0076)	0.0027 ± 0.0012 (0.0027)	0.0041 ± 0.0042 (0.0018)	0.0014 ± 0.00066 (0.0013)	0.0000105	0.008	0.0043
Zn	0.0803 ± 0.044 (0.062)	0.0309 ± 0.015 (0.0303)	0.035 ± 0.041 (0.022)	0.015 ± 0.0080 (0.014)	0.15	0.2	0.069
SO_4^{2-}	15.3 ± 3.92 (14.3)	1.58 ± 0.74 (1.57)	13.0 ± 3.83 (11.3)	0.78 ± 0.45 (0.61)	3.59	2.8	
OC	24.7 ± 9.50 (28.8)	3.61 ± 1.64 (3.78)	19.0 ± 9.58 (20.4)	2.06 ± 0.91 (1.83)	21.2	57.1	
EC	19.5 ± 8.47 (15.5)	0.82 ± 0.37 (0.86)	18.7 ± 8.50 (14.5)	0	12.1	35.2	

[a] **Mean values ± standard deviations are given with median values in parentheses for the EFECT (for TSP size).** [b] From SPECIEUROPE, Profile 154: Exhaust and road dust (PM10). [c] From SPECIEUROPE, Profile 10: Exhaust diesel and gasoline (PM10). [d] From SPECIEUROPE, Profile 140: Exhaust traffic (PM10). X_{tsp} represents the composite source profile of a mixed fleet assuming the tunnel as a traffic source and involves *rdrs*, *exh*, and *n-exh* source profiles.

Table S6. Comparison of the *exh* source profiles obtained from the EFECT and SPECIATE database.

Source	**EFECT, *exh* source profile (wt %)**	SPECIATE, *exh* source profiles (wt %) (Transportation Composite)*		
PM size	**TSP**	$PM_{2.5\text{-}10}$	PM_{10}	PM_{30}
Profile code	-	33005C	3300510	3300530
Al	0.36 ± 0.41 (0.17)	0.959	0.217	0.116
As	0.0037 ± 0.0029 (0.0038)	0	0.003	0.004
Ba	0.041 ± 0.017 (0.039)			
Be	$1.1\times10^{-4} \pm 3.4\times10^{-5}$ (1.1×10^{-5})			
Ca	0.23 ± 0.23 (0.18)	0.213	0.094	0.069

Cd	$4.2\times10^{-5} \pm 3.3\times10^{-5}$ (3.1×10^{-5})			
Cr	0.069 ± 0.021 (0.069)	0.038	0.006	0.002
Cu	0.0087 ± 0.0065 (0.0084)	0.03	0.009	0.006
Fe	0.24 ± 0.39 (0.025)	0.233	0.038	0.013
Mg	0.081 ± 0.11 (0.023)			
Mn	0.0041 ± 0.0051 (0.0027)	0.078	0.036	0.031
Ni	0.0074 ± 0.010 (0.0026)	0.017	0.003	0.001
Pb	0.0054 ± 0.011 (0.0010)	0.749	0.433	0.385
Sb	0.0017 ± 0.00090 (0.0019)			
Sn	0.0014 ± 0.00063 (0.0014)			
V	0.0041 ± 0.0042 (0.0018)	0.034	0.006	0.002
Zn	0.035 ± 0.041 (0.022)	0.125	0.064	0.056
SO_4^{2-}	13.0 ± 3.83 (11.3)			
OC	19.0 ± 9.58 (20.4)	74.9	53.8	50.1
EC	18.7 ± 8.50 (14.5)	17.3	48.3	50.9

*Developed using the steady-state vehicle exhaust profiles and no tire wear factors included, relative to the vehicle miles traveled in the Sepulveda Tunnel (Los Angeles) in 1987.

Table S7. Diagnostic ratios of selected elements for the vehicular emission sources.

		tsp	***rdrs***	***exh***	***n-exh***
Fe/Cu	Mean ± Std	82.0 ± 11.6	163	29.0 ± 10.4	154.0 ± 20.0
	Median	81.0		27.5	145.0
	Range	69.0–96.0		19.3–44.6	139.0–190.0
Ba/Cu	Mean ± Std	2.70 ± 0.40	1.56	3.73 ± 1.19	1.81 ± 0.29
	Median	2.67		3.24	1.69
	Range	2.10–3.25		2.44–5.39	1.50–2.42
Sb/Cu	Mean ± Std	0.16 ± 0.038	0.078	0.24 ± 0.063	0.076 ± 0.014
	Median	0.163		0.218	0.078
	Range	0.11–0.21		0.16–0.33	0.054–0.097
Sn/Cu	Mean ± Std	0.19 ± 0.029	0.056	0.37 ± 0.062	0.064 ± 0.0092
	Median	0.185		0.362	0.061
	Range	0.15–0.23		0.31–0.48	0.053–0.078
OC/EC	Mean ± Std	1.51 ± 0.64	6.10	0.90 ± 0.42	NA
	Median	1.56		0.78	NA
	Range	0.51–2.53		0.36–1.42	NA

Concentrations used in the diagnostic ratios were obtained from the source apportionment results of EFECT.

Table S8. Road dust resuspension (*rdrs*) and *exh* source contributions on the TSP size of the OC and EC concentrations at the receptor site.

		X_{tsp} (μg/m³)			X_{rdrs} (μg/m³)		X_{exh} (μg/m³)	*rdrs* (%)		*exh* (%)	Barbecue (%)
Date	**Day**	**OC**	**EC**	CC	OC	EC	OC	OC	EC	OC	OC
2/12/2020	Wednes-day	1.81	0.22	0.21	0.48	0.08	0.31	26.5	36.3	17.1	56.4
2/14/2020	Friday	6.61	0.61	0.45	1.03	0.17	0.86	15.5	28.0	13.0	71.5
2/15/2020	**Saturday**	12.67	1.23	0.65	1.48	0.25	1.73	11.7	20.1	13.7	74.6
2/16/2020	**Sunday**	8.02	0.53	0.5	1.14	0.19	0.75	14.2	35.8	9.3	76.5

2/17/2020	Monday	8.96	0.72	0.59	1.35	0.22	1.02	15.0	31.1	11.3	73.7
2/18/2020	Tuesday	4.79	0.66	0.58	1.32	0.22	0.93	27.6	33.4	19.4	53.0
2/19/2020	Wednes-day	4.57	0.47	0.47	1.07	0.18	0.66	23.4	38.0	14.5	62.1
2/20/2020	Thursday	7.88	1.17	0.44	1.00	0.17	1.65	12.7	14.3	20.9	66.3
2/21/2020	Friday	7.59	0.64	0.41	0.93	0.16	0.90	12.3	24.3	11.9	75.8
2/22/2020	**Saturday**	17	1.47	0.76	1.73	0.29	2.07	10.2	19.6	12.2	77.6
2/24/2020	Monday	3.66	0.46	0.37	0.84	0.14	0.65	23.0	30.6	17.7	59.2
2/25/2020	Tuesday	3.02	0.3	0.27	0.62	0.10	0.42	20.4	34.2	14.0	65.6
2/28/2020	Friday	5.18	0.48	0.32	0.73	0.12	0.68	14.1	25.3	13.1	72.8
2/29/2020	**Saturday**	9.85	0.51	0.39	0.89	0.15	0.72	9.0	29.1	7.3	83.7
3/1/2020	**Sunday**	13.68	0.45	0.46	1.05	0.17	0.63	7.7	38.8	4.6	87.7
3/6/2020	Friday	7.41	0.47	0.4	0.91	0.15	0.66	12.3	32.3	8.9	78.7
	$(X/CC)_{rdrs}$	2.28	0.38	1							
	X_{exh}/EC_{exh}	1.410	1								
	Mean ± Std	7.67 ± 4.10	0.65 ± 0.35	0.45 ± 0.14	1.04 ± 0.32	0.17 ± 0.053	0.92 ± 0.49	16.0 ± 6.24	29.5 ± 7.11	13.1 ± 4.35	71.0 ± 9.75
	Median	7.5	0.52	0.45	1.01	0.17	0.73	14.1	30.9	13.0	73.2
	Min	1.81	0.22	0.21	0.48	0.080	0.31	7.7	14.3	4.63	53.0
	Max	17	1.47	0.76	1.73	0.29	2.10	27.6	38.8	20.9	87.7

The $(X/CC)_{rdrs}$ and *Xexh*/*ECexh* are from the road dust resuspension (*rdrs*) and exhaust *(exh*) emission source profiles, respectively, for OC and EC. *Xtsp* represents the total emission.

Table S9. Method detection and quantification limits (MDL and MQL) and the percent recoveries of the elements and sulfate ions.

Element/Ion	MDL (ng/m³)	MQL (ng/m³)	Recovery (%)
Al	110	367	100.0
As	0.076	0.25	99.0
Ba	5.0	16.7	110.5
Be	0.025	0.083	106.8
Ca	190	633	97.0
Cd	0.015	0.050	102.8
Cr	11.0	36.7	113.3
Cu	1.50	5.0	91.0
Fe	115	383	93.0
Mg	14.0	46.7	95.0
Mn	0.95	3.2	97.0
Ni	3.50	11.7	95.5
Pb	0.32	1.1	97.0
Sb	0.017	0.057	90.8
Sn	0.11	0.37	90.0
V	0.31	1.03	104.2
Zn	8.80	29.3	94.0
*SO_4^{2-}	0.95	3.17	97.3
**OC	0.20	0.67	105
**EC	0.04	0.13	NA

NA: Not applicable. There is no SRM or reference sample for elemental carbon. * In unit of μg/mL. ** In unit of μg C/m³.

Method detection limits were calculated from ten replicates of the lowest level calibration standard (1.0 μg/L) solution. LOD values were three times the standard deviation

of ten replicates, and the LOQ values were calculated from ten times the standard deviation of ten replicates. Then, the LOD and LOQ values were converted into the method detection and quantification limits.

For the recovery calculations of the elements NIST SRM 1648a and SRM 1649a, urban dust were used. Recovery of sulfate was determined by using the ERM-CA408 simulated rainwater standard. For the OC, standard sucrose samples were used as the reference material.

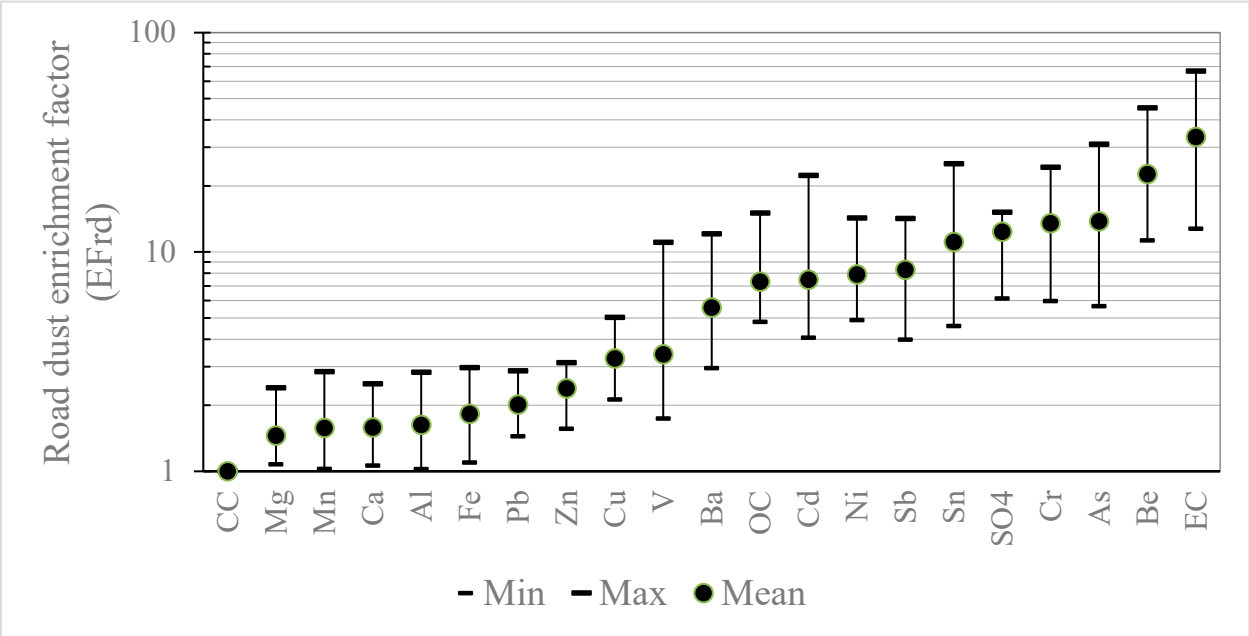

Figure S1. Mean road dust enrichment factors of the elements in the tunnel atmosphere relative to the TSP fraction of the tunnel road dust.

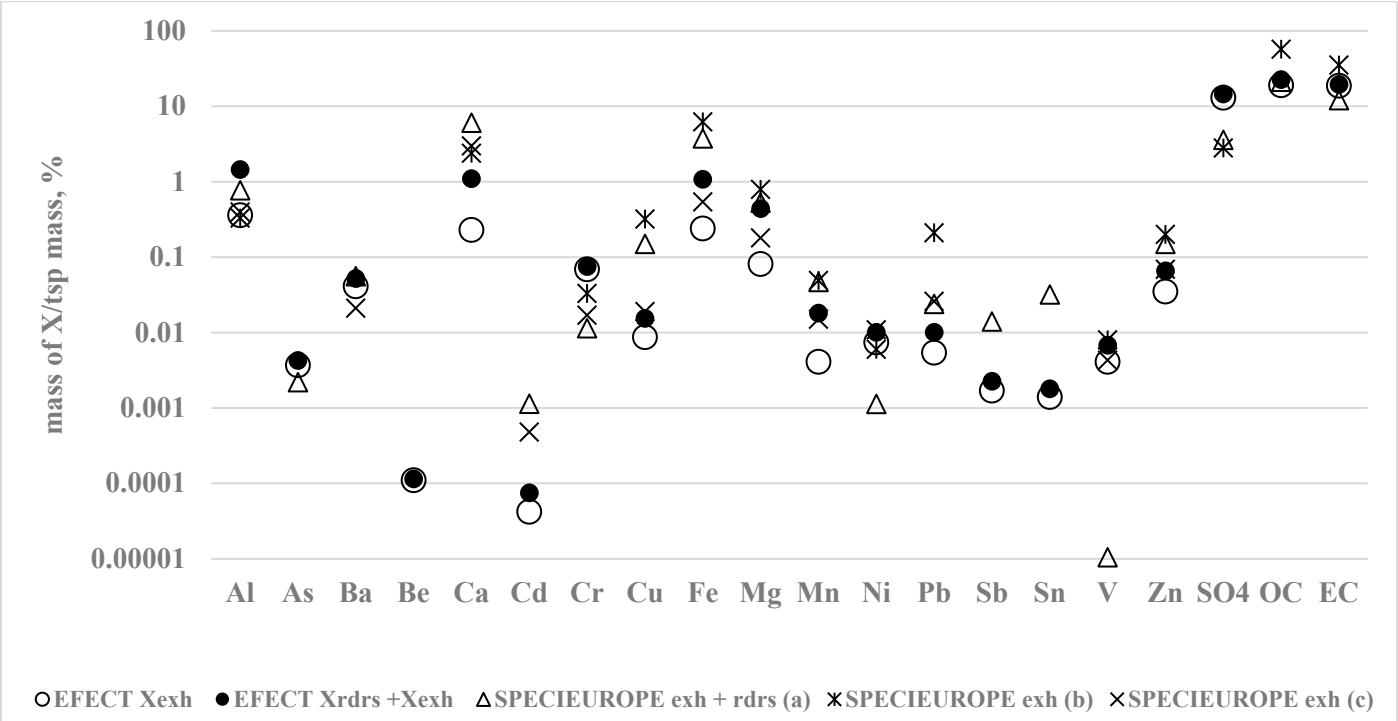

Figure S2. Real-world *exh* source profiles (mass of element to tsp mass) for a mixed fleet obtained from the EFECT method and a comparison with the SPECIEUROPE source profiles (%). [a] Profile 154: Exhaust and road dust (PM10), [b] Profile 10: Exhaust diesel and gasoline (PM10), [c] Profile 140: Exhaust traffic (PM10).

File S1. The First Stage of the EFECT: Road Dust Enrichment Factors, EFrd (EF)

Almost all of the studies in the literature have used continental, regional, or local crustal compositions as background soil composition in EF calculations [8,13,50,51] to assess the degree of contamination by anthropogenic emission sources. In contrast, we used the same approach with contaminated background soil, which was tunnel road dust. Our purpose in this study was not to determine the degree of contamination but to quantify the elemental contributions from the road dust resuspension. For this purpose, we normalized the road dust source profile (μg X/g road dust) with the concentration of road dust CC (μg CC/g road dust), and the net concentrations of elements (X_{tsp}) to CC_{tsp} ratio to calculate the road dust EF. The road dust enrichment factors, EFrd, for the elements were calculated from the below equation (Equation (S1)). The mean road dust enrichment factors and the corresponding minimum and maximum values were presented in Figure S1.

$$〖EF〗_rd=((〖[X]〗_tsp/〖[CC]〗_tsp))/(([X]_rd/[CC]_rd)) \quad \text{(S1)}$$

where EF_{rd} is the enrichment factor with respect to the background tunnel road dust. Concentration (X) refers to the net concentrations of measured species in the TSP samples and the mean concentrations of elements in the road dust. The concentration (CC) refers to the net concentration of the reference element, carbonate carbon, in the TSP samples and the mean concentration of CC in the background road dust.

The enrichment factor technique requires the normalization of measured concentrations of elements with respect to a reference or a normalizing element that must be stable and representative of the reference soil used, and its concentration should not be altered in time [52]. We experimentally showed that the ratio of measured species to CC in road dust stayed almost constant for more than a year. According to the information provided by the Bolu Mountain Highway Tunnel Maintenance and Operation Unit, the tunnel road surface and the sidewalks are washed with pressurized water 3 to 4 times a year, depending on the level of dust monitored automatically in the tunnel atmosphere. Therefore, the first sampling campaign (2018) was carried out two months later than the tunnel wash. The second sampling, the 2019 campaign (road dust sampling only), was carried out 13 months after the first campaign, and 3 months after the tunnel wash. The results of the analyses of the resuspended road dust samples corresponding to two different sampling campaigns were evaluated and compared to determine the compositional changes that might be caused due to tunnel wash and time. The mean concentrations of the measured species and their CC ratios corresponding to the 2018 and 2019 campaigns are presented in Table S2. The study area is a rural site that is covered with vegetation, and there are no significant known anthropogenic emission sources around. Results showed that the CC normalized values of the measured species (i.e. road dust source profile) did not change significantly with time and tunnel washing activities when compared to the changes observed in the mean elemental concentrations corresponding to the 2018 and 2019 campaigns. As additional support to this claim, the CC concentrations in the road dust samples that were collected at the same sampling points in 2014, [10], 2018 [8], and 2019 are shown. The mean and the standard deviations of road dust CC concentrations in 2014, 2018, and 2019 were 50300 ± 2170, 46500 ± 2940, and 50700 ± 3800 μg/g, respectively. The mean concentration of CC in 2014 was quite similar to the result obtained in 2019, corresponding to about a five-year time interval. Furthermore, it was reported that the road dust composition had not been altered due to the tunnel ventilation rates [17,19] and street washings [53]. Therefore, it is clear that for short-term sampling campaigns, the tunnel road dust and its CC content can safely be used as a background soil and normalizing/reference element, respectively, to estimate the elemental contributions from the rdrs source.

CC concentrations in both the road dust and the TSP samples were determined from the OC/EC measurement method [10,54]. It is known that the carbonate carbon (from $CaCO_3$) is volatilized at the end of the first non-oxidizing heating cycle and appears as the OC4 peak (CC peak). Then, the flame ionization detector (FID) response for the CC peak

was integrated and subtracted from the OC. Following this information, we quantified the CC concentrations by re-integration of the OC4 peaks present in the sample thermograms manually [55]. The EF_{rd} results presented in Figure S1 support the use of CC as the road dust reference element since no species had EF_{rd} values lower than CC, or unity.

It should be noted that for a non-rural site or an arid region, the tunnel road dust must be corrected against the local soils first, and then the resultant composition should be used as the background road dust. For example, dust incursions in arid regions and/or any industrial emission at the receptor site can alter the road dust composition, which can lead to significant errors in the source apportionment results.

Our trials during the method development stages showed that in the absence of CC data, the road dust content of crustal elements (Si, Al, Ca, Mg, and Fe) can also be used as reference elements, even if they have additional sources such as exhaust and non-exhaust emissions. However, for this study, there was an enrichment risk of road dust with Ca due to the usage of calcium salt (calcium chloride) as a road de-icing agent, together with sodium chloride. Similarly, the Si could not be used as a reference element since it was the main filter material and was not measured in this work. Other major crustal elements such ass aluminum (Al), iron (Fe), and magnesium (Mg) may be used as reference elements with some degree of uncertainty compared to CC. Al, Fe, and Mg are abundant in road dust due to contributions from local soils, exhaust and non-exhaust vehicular emissions, and abrasion/degradation of the concrete structures and furniture in the tunnel. The tail-pipe and non-exhaust emissions (without considering road dust resuspension contribution) of these crustal elements may create additional uncertainties in the quantification of source contributions since diesel fuels and lubricating oils contain significant amounts of Al, Fe, and Mg. The sources of these elements are due to their presence in diesel fuels and lubricating oils whether naturally or as components of additives [13,24,25]. Furthermore, the wear metals are the main sources of Al (from pistons and additives) and Fe (from cylinder liner, valves, shaft, and camshaft) [47].

In this study, even though we used contaminated soil (i.e., road dust at the sampling site) as the background matrix, we saw that for an element, as the contribution of exhaust emission increased, the EF_{rd} value of that element also increased. Using this observation, we decided to group the elements according to their EF_{rd} values. Consequently, the EF values between 1.0 and 2.0 were considered non-enriched in the tunnel TSP samples and evaluated as the road dust element, which mainly came from the road dust resuspension. While the elements with EF values $2 \leq EF < 10$ were evaluated as enriched, the elements with EF values equal to 10 and higher were evaluated as highly enriched in the tunnel TSP samples. The road dust enrichment factors of the elements indicated that the first group of five elements including Mg, Mn, Ca, Al, and Fe are mainly associated with a source derived from road dust. On the other hand, the elements including Pb, Zn, Cu, V, Ba, OC, Cd, Ni, and Sb were enriched, which means that these elements were contributed significantly by the emission (*em*) sources (exhaust and non-exhaust). Tin, sulfate ion, Cr, As, Be, and EC had the highest EF values, which showed that these species were contributed mainly by the exhaust emissions, rather than road dust resuspension and the non-exhaust emissions (see Figure 1 and Figure S1(or Table S3).

File S2. The second stage of EFECT: Exhaust EC tracer method (ECT)

The emission (*em*) source, in this method, involves the exhaust and non-exhaust emissions, as mentioned before. In a tunnel atmosphere, the elemental carbon (EC) in PM samples, TSP in this study, (EC_{tsp}) has only two main sources, namely, road dust resuspension (EC_{rdrs}) and the exhaust emissions (EC_{exh}). Since the concentrations of EC and other measured species contributed by the outside atmosphere were assumed to be corrected by subtracting the inlet concentrations from the outlet concentrations. The primary pollutant EC is an incomplete combustion product of fuels and therefore, after correcting against *rdrs* contribution, exhaust emission becomes the main emission source of EC in the tunnel atmosphere. Then the concentration of EC from the emissions (EC_{em}) will be equal to EC_{exh}.

Then EC_{exh} can be computed from the difference between the EC_{tsp} and EC_{rdrs} (Eq. (4)). However, in the case of other elements (X), the X_{em} equals the sum of X_{exh} and $X_{n\text{-}exh}$. In this case, there are two unknowns (X_{exh} and $X_{n\text{-}exh}$) but a single equation. Therefore, an additional equation is required. To overcome this problem we tried to construct a mathematical linear relationship between the X_{exh} and EC_{exh}. To relate X_{exh} and EC_{exh}, we proposed dimensionless equality to get Eq. (6). In the equality, we normalized X_{exh} and EC_{exh} with their emission components, X_{em} and EC_{em}, respectively. The resultant ratios were re-normalized with the ratios of X_{em}/X_{tsp} and EC_{em}/EC_{tsp} for X and EC, respectively, to include all the possible synergetic contributions to the magnitude of X_{exh}. The numerator, (〖EC〗_exh/ 〖EC〗_(tsp- 〖EC〗_rdrs)), in the equality is the ratio of EC_{exh} to EC_{em} and equal to unity, however, the term, *(X_exh/X_(tsp- X_rdrs)*) can be equal to or smaller than 1.0 due to the presence of *n-exh* contributions for most of the elements.

((X_exh/X_(tsp- X_rdrs)))/((X_(tsp- X_rdrs)/X_tsp)= ((〖EC〗_exh/ 〖EC〗_(tsp- 〖EC〗_rdrs)))/((〖EC〗_(tsp- 〖EC〗_rdrs)/ 〖EC〗_tsp))) (S2)

Where, (X_{tsp} - X_{rdrs}) = X_{em}, and (EC_{tsp} - EC_{rdrs}) = EC_{em}, as mentioned above. We confirmed the equality and obtained y = x, R2 = 1.0, using the elemental concentrations available in this work. Following the confirmation of the equality in Eq. (S2), we extracted X_{exh} to get Eq. (6).